# Critical Velocity of Fluidelastic Vibration in a Nuclear Fuel Bundle

**Sang Nyung Kim*, Sung Yup Jung**
*Department of Nuclear Engineering, Kyunghee University*

In the core of the nuclear power plant of PWR, several cases of fuel failure by unknown causes have been experienced for various fuel types. From the common features of the failure pattern, failure lead time, flow conditions, and flow induced vibration characteristics in nuclear fuel bundles, it is deduced that the fretting wear failure of the fuel rod at the spacer grid position is due to the fluidelastic vibration. In the past, fluidelastic vibration was simulated by quasi -static semi-analytical model, so called the static model, which could not account for the interaction between the rods within a bundle. To overcome this defect and to provide for more flexibilities applicable to the fuel bundle, Tanaka's unsteady model was modified to accomodate the geometrical differences and governing parameter changes during the operations such as the number of rods, pitch to diameter ratio (P/D), spring force, damping coefficient, etc. The critical velocity was calculated by solving the governing equations with the MATLAB code. A comparison between the estimated critical velocity and the test result shows a good agreement. Finally, the level of decrease of the critical velocity due to the reduction in the spring force and reduced damping coefficient due to the radiation exposure is also estimated.

**Key Words** : Critical Velocity, Fluidelastic Vibration, Flow-induced Vibration, Fuel Bundle, Damping, Stiffness

**Nomenclature**

| | |
|---|---|
| C | : Coefficient of fluid force |
| $C_m$ | : Added mass coefficient (dimensionless) |
| $C_D$ | : Damping coefficient (dimensionless) |
| $C_k$ | : Stiffness coefficient (dimensionless) |
| D | : Fuel rod diameter |
| Da | : Damping coefficient |
| F | : Fluid dynamic force |
| $f$ | : Rod frequency in the fluid |
| $K_C$ | : Fuel cladding stiffness |
| $K_S$ | : Spring stiffness |
| m | : Equivalent mass per unit length |
| P | : Fuel rod pitch |
| $V_R$ | : Reduced velocity ($V/fD$) |
| V | : Gap velocity |
| X | : Fuel rod displacement |
| $\dot{X}$ | : Derivation of X with respect to time |
| $\rho$ | : Fluid density |
| $\lambda$ | : Eigenvalues |

* Corresponding Author,
**E-mail** : snkim@nms.kyunghee.ac.kr
**TEL** : +82-31-201-2564 ; **FAX** : +82-31-202-1541
Department of Nuclear Engineering, Kyunghee University, Seocheon-ri #1, Kiheung-up, Youngin-si, Kyunggi-do 449-701, Korea. (Manuscript **Received** November 23, 1999; **Revised** May 26, 2000)

## 1. Introduction

Many types of industrial plants such as the heat exchangers, boilers, and cores of nuclear power plants contain the rod bundle as a component. The bundle is usually subjected to high velocity flow to enhance the heat-transfer. Also, in case of the nuclear fuel bundle (F/B), it is desirable to minimize structural support to reduce the core volume, pressure drop, and improve on the neutron economy. So they are very vulnerable to fretting wear due to the flow induced vibration (FIV). In particular, the F/B is exposed to hostile conditions such as high temperature and pressure, high speed flow, intense radiation bombardment, fuel cladding creep, spring force reduc-

tion, among others. In the last decade, there have been many cases of the nuclear fuel failure by fretting wear reported in many plants for various type of nuclear fuel with mixing devices; mixing vane and intermediate flow mixer. The FIV was blamed for these failures. However, the exact mechanism involved was not clear. Although the damage does not pose a serious safety problem in the nuclear power plants, it can be guite costly due to plant shutdowns and radioactive waste production.

Typical FIV categories include fluidelastic vibration, periodic shedding, turbulence induced excitation, and acoustic resonance(Pettigrew et al., 1991). Even though all these mechanisms could be present in the rod bundle during normal operations, excessive vibration is primarily induced by one of these mechanisms depending on the operating conditions. As mentioned before, due to the hostile thermal hydraulic conditions and structural complexity of the F/B, it is very difficult to pinpoint the cause of a fuel failure. By an exhaustive review of the plant operating experiences, failure patterns, thermal hydraulic and structural characteristics of the F/B, the cause finally was boiled down to the fluidelastic vibration(Jung and Kim, 1998).

The fluidelastic vibration was studied by many scientist. B. W. Robert found the fluid dynamic forces induced by jet switch(Blevins, 1977) and pointed out the possibility of fluidelastic vibration of tube bundles. H. J. Connors conducted a model test with single-row cylinders supported by elastic spars in cross flow. He found that the cylinders started to vibrate abruptly at a certain velocity. The vibration occurred when the energy supplied in one cycle was greater than the energy dissipated by structural damping.

H. Tanaka calculated the critical velocity of the fluidelastic vibration based on the unsteady fluid dynamic force in a tube bundle. In Tanaka's model, the interactions between the rods in a given bundle are particularly considered. Also the interaction coefficients were experimentally determined(Tanaka and Takahara, 1980). Particularly, his model predicted significant vibrations in the second layer, which can be well correlated with the nuclear fuel failure patterns mentioned in the next section.

Therefore in this study, Tanaka's model is adopted and modified to calculate the critical velocity by taking account of the unsteady fluid dynamic force, spring force deflection by radiation exposure, and fuel cladding creep.

## 2. Overview of Vibration Mechanisms

As mentioned before, four FIV mechanisms can be relevant to the vibration of the rod bundle components. The relative predominance of these mechanisms for different flow situations is outlined in Table 1(gettigrew et al., 1991). For various flow conditions of the core, the relevant mechanisms are darkened as shown in Table 1.

## 3. Operating Experiences (Failure Patterns)

Since the F/B has a complex structure and is

**Table 1** Summary of flow condition of FIV

● ; most important, ○ ; important, × ; unlikely

| Flow situation | Fluidelastic vibration | Periodic shedding | Turbulence excitation | Acoustic resonance |
|---|---|---|---|---|
| Axial-flow | | | | |
| Internal | | | | |
| Liquid | × | × | ● | ○ |
| Gas | × | × | ○ | ● |
| Two phase flow | × | × | ● | × |
| External | | | | |
| Liquid | × | × | ● | × |
| Gas | × | × | ○ | ○ |
| Two phase flow | × | × | ● | × |
| Cross-flow | | | | |
| 1-cylinders | | | | |
| Liquid | | | | |
| Gas | × | ● | ● | × |
| Two | × | ○ | ○ | × |
| phase flow | × | × | ● | × |
| Tube bundle | | | | |
| Liquid | ● | × | ○ | × |
| Gas | ● | × | ○ | ● |
| Two phase flow | ● | × | ● | × |

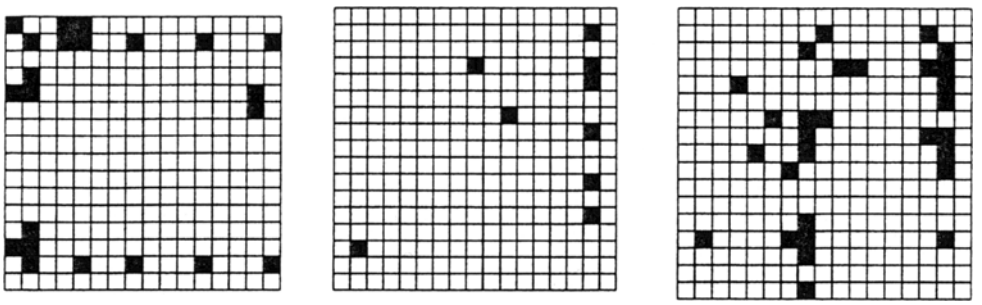


**Fig. 1** The position of failed rods in the F/B

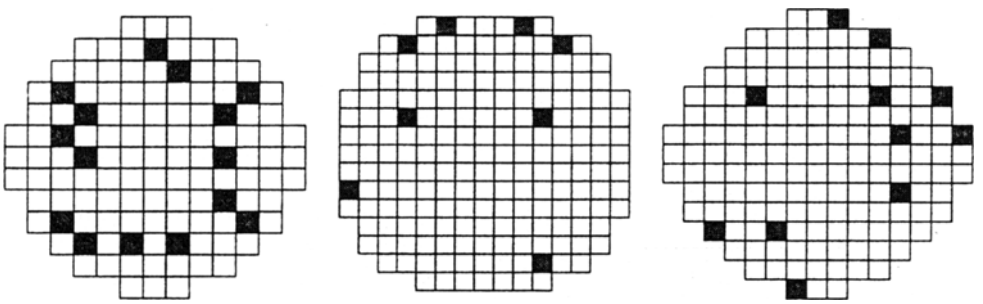


**Fig. 2** The position of failed F/B in the core

operated in severely hostile conditions of high temperature, pressure, and high radiation exposure, many things can cause the fuel rod to vibrate. However, the cause of failure is deemed to be the FIV in the case for the reasons mentioned previously.

In general, it was known that the vibration of the F/B was mainly induced by the axial flow. However, the failed F/Bs have a mixing vane whose purpose is to enhance the heat transfer by the cross-flow mixing. The enhanced cross flow can cause the vibration and result in the fuel rod failure.

Figures 1 and 2 show the typical failure patterns of the fuel rod by the FIV. As shown in Figue 1, the fuel rods are arranged in a square lattice. Figures 1 and 2 show a pseudo fuel assembly and a core consisting of failed fuel rods or assemblies from various assemblies or cores by putting in an assembly or a core. Figure 2 also shows the core loading patterns and the failed assemblies in the core. From the failed fuel inspection results, the following conclusions can

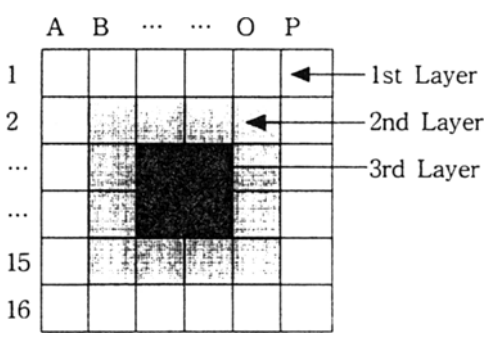


**Fig. 3** The definition of the layer

be drawn.

First, the fretting wear in a rod takes place at the center of the space grid (spring) location. Also the damage needs a long lead time. It is quite different from the characteristics of a turbulence excited vibration which induces failure at the inlet and the outermost region in the F/B, that is, at the location subjected to strongest turbulence excitation. Therefore it can be concluded that the turbulence excitation is not the predominant mechanism for the rod damage. Second, as shown

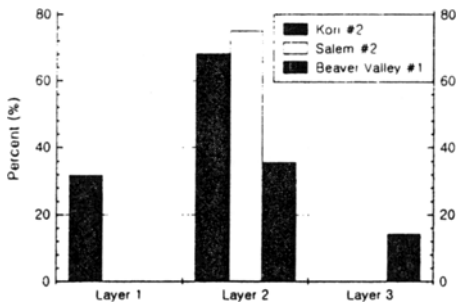


**Fig. 4** The failure frequency in each layer

in Fig. 4, the location of the damaged rods in the F/B is concentrated on the 2nd layer defined in Fig. 3. This tendency can only be explained by a unique characteristic of the fluidelastic vibration. This characteristic that the amplitude of the tubes in the 2nd layer is the largest among all layers was verified by Tanaka's experiment(Tanaka and Takahara, 1981). Third, the irregularity of the damaged locations in the core is observed. It is different from the periodic vortex shedding which leads to symmetrical failure of the rods, because the core has symmetric flow condition.

From these reasons, it is concluded that the fluidelastic vibration may be the governing mechanism for the fuel rod damage.

## 4. Vibration Modeling

The vibration equation was derived for the center rod(O) by applying the force balance. The unsteady fluid dynamic force applied to the rod by the vibrations, consists of three types of forces; the inertia force due to added fluid mass, damping force due to fluid, and stiffness force due to the rod displacement(Tanaka and Takahara, 1981).

$$F=\frac{\rho D^2}{2}C_m\ddot{X}+\frac{\rho DV}{2}C_D\dot{X}+\frac{\rho V^2}{2}C_kX \qquad (1)$$

For steady state vibration, Eq.(1) can be reduced as follows:

$$\begin{aligned}F&=\frac{1}{2}\rho V^2[-C_m((2\pi fD)^2/V^2)\\&\qquad+iC_D(2\pi fD/V)+C_k]X\\&=\frac{1}{2}\rho V^2[-4\pi^2C_m/V_R^2+i2\pi f/V_R+C_k)X\\&=\frac{1}{2}\rho V^2C(V_R)X \qquad (2)\end{aligned}$$

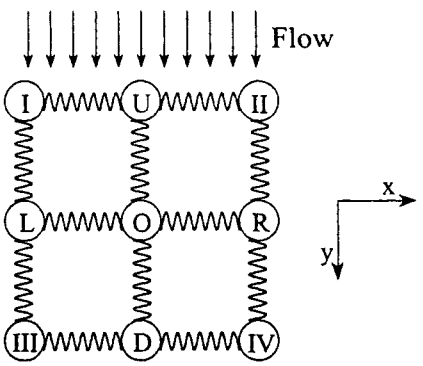


**Fig. 5** Geometrical model of fuel rod

As can be shown from Eq.(2), the fluid dynamic coefficient $C(V_R)$ is a complex number dependent upon the reduced velocity($V_R$).

The fluid dynamic forces are induced not only by the vibration of the rod itself (O), but also by the vibration of the adjacent fuel rods. However, the effect of the diagonal rods( I , II, III, IV) was neglected because the distance between I and O is much larger than that between L and O. Therefore the fluid dynamic force acting on the center rod per unit length can be qiven by

$$F_X=\frac{1}{2}\rho V^2\sum_{k=1}^{5}(C_{Xk\mathrm{X}}X_k+C_{Xk\mathrm{Y}}Y_k) \qquad (3)$$

$$F_Y=\frac{1}{2}\rho V^2\sum_{k=1}^{5}(C_{Yk\mathrm{Y}}X_k+C_{Yk\mathrm{Y}}Y_k) \qquad (4)$$

where $k=1\sim5$ denote the five rods (O, L, R, U, D) shown in Fig. 5. $C_{XjX}$'s are the fluid dynamic force coefficients, and the first, second and third suffixes denote the direction of the force, the position of the vibrating fuel rod, and the direction of vibration, respectively(Tanaka and Takahara, 1980). Because of the symmetry of the fuel rod arrangement and flow direction, the fluid dynamic force $F_{YOX}$ is symmetric and it's derivative is zero. $F_{YUX}$, $F_{YDX}$, $F_{XOY}$, $F_{XDY}$, and $F_{XUY}$ are also symmetric, and their derivatives are all zero. The following relations for the fluid dynamic coefficients can be deduced

$$\begin{aligned}&C_{YUX},\ C_{YDX},\ C_{XOY},\ C_{YOX},\ C_{XUY},\ C_{XDY}=0\\&C_{XRX}=C_{XLX}\quad C_{YRY}=C_{YLY}\\&C_{XRY}=-C_{XLY}\quad C_{YRX}=-C_{YLX}\end{aligned} \qquad (5)$$

The fluid dynamic force Eqs. (3) and (4) can be reduced by the relations mentioned above in

the following manner:

$$F_X=\frac{1}{2}\rho V^2[C_{XOX}X_O+C_{XLY}(X_L+X_R)+C_{XLY}(Y_L-Y_R)+C_{XUX}X_U+C_{XDX}X_D] \quad (6)$$

$$F_Y=\frac{1}{2}\rho V^2[C_{YOY}Y_O+C_{YLX}(X_L-X_R)+C_{YLY}(Y_L+Y_R)+C_{YUY}Y_U+C_{YDY}Y_D] \quad (7)$$

Let the X-direction and Y-direction be expressed by suffixes of odd and even numbers, respectively.

However, Tanaka's model could not account for the irradiation condition. To overcome this defect, the stiffness force is divided into cladding and grid spring stiffness forces. The change of the grid spring stiffness force by irradiation is taken into account in our calculation.

Then the equation of motion for the rod can be written as follows.

$$m_{sj}\ddot{X}_j+D_{asj}\dot{X}_j+(K_C+K_S(T))X_j=F_j \quad (8)$$

As mentioned previously, the fluid dynamic forces arise from the inertia of the added mass, damping, and stiffness forces of the fluid. Therefore, Eq. (8) can be written as follows:

$$m_{sj}\ddot{X}_j+D_{asj}\dot{X}_j+(K_C+K_S(T))X_j=\frac{1}{2}\rho D^2\sum_{k=1}^{5}C_{mjk}\ddot{X}_{jk}+\frac{1}{2}\rho DV\sum_{k=1}^{5}C_{Djk}\dot{X}_{jk}+\frac{1}{2}\rho V^2\sum_{k=1}^{5}C_{Kjk}X_{jk} \quad (9)$$

$$m_{sj}\ddot{X}_j+D_{asj}\dot{X}_j+K_{sj}X_j=\sum_{k=1}^{5}(m_{fjk}\ddot{X}_{jk}+D_{fjk}\dot{X}_{jk}+K_{fjk}X_{jk}) \quad (10)$$

where suffixes f, s, and k denote fluid, fuel rod, and five rods around the central rod(j=O), respectively. The three fluid dynamic forces could be expressed by multiplying the corresponding coefficients and phase differences as follows.

$$m_{fjk}\ddot{X}_j=\frac{1}{2}\rho D^2C_{mjk}\ddot{X}_k \quad (11)$$

$$D_{fjk}\dot{X}_k=\frac{1}{2}\rho DVC_{Djk}\dot{X}_k=\frac{1}{2}\rho DVC_{Djk}\sin\phi\dot{X}_k \quad (12)$$

$$K_{fjk}X_k=\frac{1}{2}\rho V^2C_{Kjk}X_k=\frac{1}{2}\rho V^2C_{Kjk}\cos\phi\dot{X}_k \quad (13)$$

Equations (11) to (13) are reduced to the following simple form.

$$m_{fjk}\ddot{X}_j+K_{fjk}X_k=\frac{1}{2}\rho V^2(C_{Kjk}\cos\phi-\frac{4\pi^2}{V_R^2}C_{mjk})X_k \quad (14)$$

The phases and the coefficients in Eqs.(12) and (14) can be obtained from the experimental works(Tanaka and Takahara, 1981). Therefore the equation for the whole of the F/B can be written in the matrix form as follows:

$$[m](\ddot{X}_j)+[D](\dot{X}_j)+[K](X_j)=0 \quad (15)$$

Equation (15) gives a set of simultaneous equations for {X}. If the solution is $X=X_0e^{\lambda t}$, Eq. (15) can be expressed as follows

$$\begin{bmatrix} m\lambda+D & K \\ I & -\lambda I \end{bmatrix}\begin{pmatrix}\dot{X}\\ X\end{pmatrix}=0 \quad (16)$$

The eigenvalues $\lambda$ can be obtained by solving Eq. (16). If $\lambda$R, which is the real part of $\lambda$, is positive, the vibration in the corresponding mode is unstable and the amplitude increases with time. If $\lambda$R is negative, the vibration mode is stable. So the critical velocity is defined as the velocity at which the value of $\lambda$R becomes zero.

## 5. Effects of Parameter Changes on the Critical Velocity

The mechanical properties such as the damping coefficient and spring stiffness can be affected by the irradiation and the weight of the fuel rod during transportation. The change of the spacer

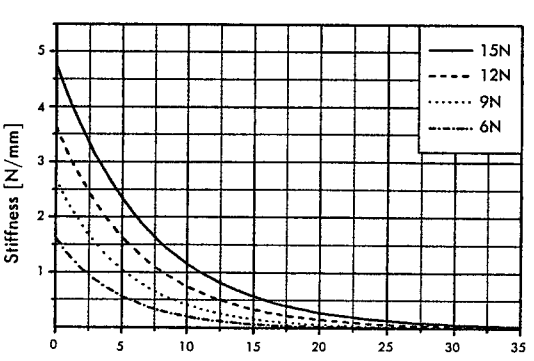


**Fig. 6** Reduction of spring stiffness at 5th spacer grid

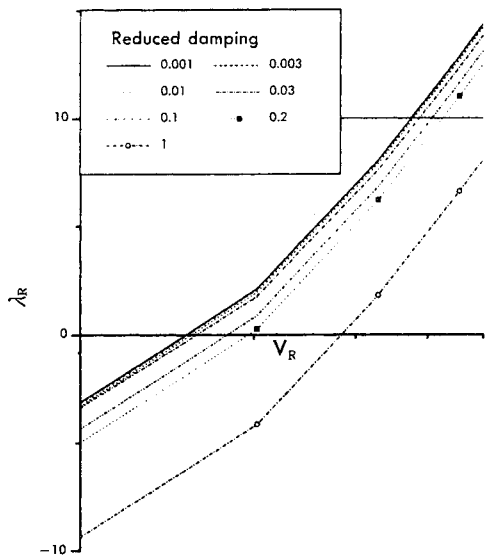


**Fig. 7** Real part vs critical velocity under unirradiated condition

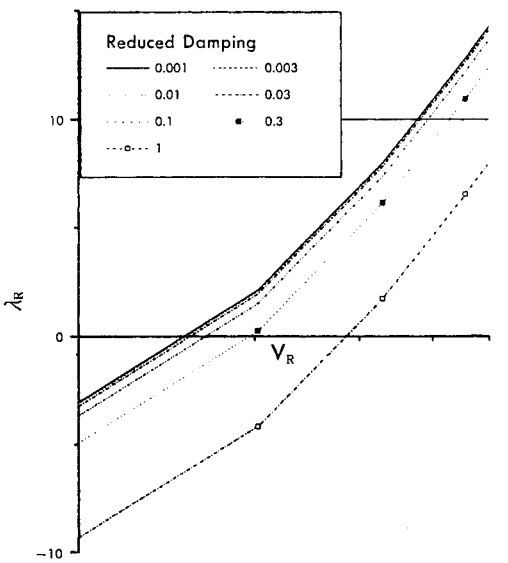


**Fig. 8** Real part vs critical velocity under irradiated condition (33MWD/KGU)

grid stiffness by irradiation (including the initial stiffness change during transportation) is shown in Fig 6 which was calculated from the KAERI report (1996). The change in the damping coefficient by the operation environment was not yet known specifically. So the effect of the damping coefficient on the critical velocity was analyzed by sensitivity calculation of damping coefficient.

## 6. Numerical Results and Discussion

For the sensitivity analysis of the damping coefficient, the real parts of eigenvalues were calculated by increasing the reduced velocity for 3×3 rod bundle which has a height of 300mm, diameter of 30mm, and pitch to diameter ratio of 1.33 immersed in 20℃ water. The calculations were executed for both the unirradiated and irradiated (33MWD/KGU) conditions (Figs. 7, 8). The results were fitted by a 4th order polynomial. As mentioned above, the critical velocity is determined when the value of $\lambda R$ is zero.

The results for unirradiated condition are compared with the experimental data for 4×7 bundle, and Connor's model (cross flow, P/D=1.47, K=4.0, n=0.5) (Fig. 9). The comparison

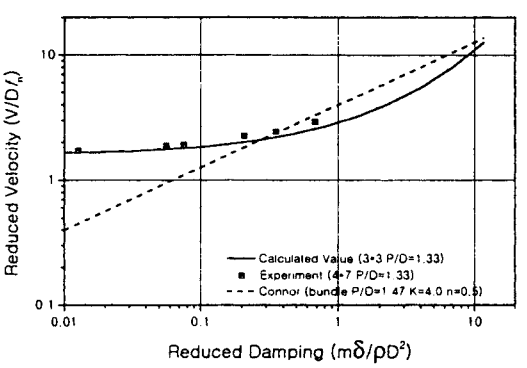


**Fig. 9** Comparison of critical velocity between measured, calculated, and predicted values

shows a good agreement with the experimental data. To verify the validity of the modified model for the irradiated rod, the calculated results are to be compared with the critical velocity based on the cross flow of KORI #2. In the case of the Kori #2 F/B, the cross flow velocity and frequency are 27~31cm/sec and 18~20Hz, respectively. When this condition is applied to the proposed model, the reduced damping coefficient should be larger than 0.0037~0.0129, the precise value being dependent on the velocity and frequency. The calculated values fall within the typical range of the reduced damping coefficient for the rod bundle which is 0.0001~0.05. Figure 10 illustrates

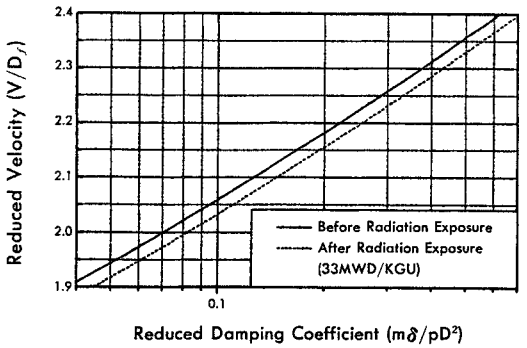


**Fig. 10** Comparison of the predicted critical velocities with and without radiation exposure

the change in the critical velocity after irradiation.

The critical velocity is reduced by 3.3% after the radiation exposure. In particular, the result showed that the effect of radiation exposure are more significant at the reduced damping 0.1～10.0. The decrease in the critical velocity resulted from the decrease in the grid stiffness under the irradiation condition. However, the decrease in the mass damping parameter due to the irradiation is not included in the present calculation.

## 7. Conclusions

After a comprehensive review of the general characteristics of the flow induced vibrations, the flow conditions for these vibrations, striking features of the failure by these vibrations, the failure pattern, and flow conditions in the fuel assembly, it was concluded that the recent fuel failures by fretting wear are caused by the fluidelastic vibration. The observed vibration had a characteristic that the most signigicant vibration occurred in the second layer of the rod bundle.

From the force balance for the rod in the flow field, a set of simultaneous equations for the fluidelastic vibration was derived that accounted for the interactions between the neighboring rods. The derived simultaneous equation was modified to accommodate reduced spring force, the fuel material property changes such as the damping coefficient, rod stiffness, and the fuel rod cladding creep by high temperature operating conditions and irradiation. The critical velocity at which the real part of the eigenvalue is zero is calculated by the MATLAB. The critical velocity decreases as the spacer grid stiffness is reduced by the radiation exposure. In particular, the critical velocity was greatly affected by the reduced damping coefficient in the range of 0.1～10.0.

For more accurate calculation, the level of decrease of the damping coefficient by irradiation should be specifically determined.

## 8. Acknowledgment

This research was supported by Korean Institute of Science and Technology Evaluation and Planning. This support is gratefully acknowledged.

## References

Blevins, R. D., 1977, Flow-Induced Vibration, Van Nostrand Reinhold Company

Jung, S. Y., Kim, S. N., 1998, "Analyze Fluidelastic Vibration of Nuclear Fuel Assembly," *Proceedings of Nuclear Thermal Hydraulic and Safety*, Vol. 1, pp. 180～184.

KAERI, 1996, Analysis of the cause for the KORI #2 fuel failures, KAERI report.

Paidoussis, M. P., 1981, "Fluidelastic Vibration of Cylinder Arrays in Axial and Cross Flow State of the Art," *Journal of Sound and Vibration, Vol.* 76, No. 3, pp. 329～360.

Pettigrew, M. J., Carlucci, L. N., Taylor, C. E., and Fisher, N. J., 1991, "Flow-Induced Vibration and Related Technologies in Nuclear Components," *Nuclear Engineering and Design*, Vol. 131, 81～100.

Tanaka, H. and Takahara, S., 1980, "Unsteady Fluid Force on Tube Bundle and Its Dynamic Effect on Vibration," *Flow-Induced Vibration of Power Plant Component ASME Special Publication* PVP-41, pp. 77～92.

Tanaka, H. and Takahara, S., 1981, "Fluid Elastic Vibration of Tube Array in Cross Flow," *Journal of Sound Vibration,* Vol. 77, No. 1, pp. 19～37.